Molecular Cancer Therapeutics

Fluorouracil Enhances Photodynamic Therapy of Squamous Cell Carcinoma via a p53-Independent Mechanism that Increases Protoporphyrin IX levels and Tumor Cell Death

Sanjay Anand[1,2], Kishore R. Rollakanti[1], Nikoleta Brankov[1], Douglas E. Brash[3], Tayyaba Hasan[4], and Edward V. Maytin[1,2,4]

Abstract

Photodynamic therapy (PDT), using 5-aminolevulinic acid (ALA) to drive synthesis of protoporphryin IX (PpIX) is a promising, scar-free alternative to surgery for skin cancers, including squamous cell carcinoma (SCC) and SCC precursors called actinic keratoses. In the United States, PDT is only FDA approved for treatment of actinic keratoses; this narrow range of indications could be broadened if PDT efficacy were improved. Toward that goal, we developed a mechanism-based combination approach using 5-fluorouracil (5-FU) as a neoadjuvant for ALA-based PDT. In mouse models of SCC (orthotopic UV-induced lesions, and subcutaneous A431 and 4T1 tumors), pretreatment with 5-FU for 3 days followed by ALA for 4 hours led to large, tumor-selective increases in PpIX levels, and enhanced cell death upon illumination. Several mechanisms were identified that might explain the relatively improved therapeutic response. First, the expression of key enzymes in the heme synthesis pathway was altered, including upregulated coproporphyrinogen oxidase and downregulated ferrochelatase. Second, a 3- to 6-fold induction of p53 in 5-FU–pretreated tumors was noted. The fact that A431 contains a mutant form p53 did not prevent the development of a neoadjuvantal 5-FU effect. Furthermore, 5-FU pretreatment of 4T1 tumors (cells that completely lack p53), still led to significant beneficial inductions, that is, 2.5-fold for both PpIX and PDT-induced cell death. Thus, neoadjuvantal 5-FU combined with PDT represents a new therapeutic approach that appears useful even for p53-mutant and p53-null tumors. *Mol Cancer Ther; 16(6); 1092–101. ©2017 AACR.*

Introduction

Photodynamic therapy (PDT) is a noninvasive cancer treatment in which a prodrug, either 5-aminolevulinic acid (ALA) or its methyl ester (MAL) is selectively taken up by neoplastic cells and converted within mitochondria into protoporphyrin IX (PpIX), which sensitizes the cells to visible light (1). PpIX becomes photoactivated and creates free radical species in the presence of oxygen, thereby killing the cancer cells. PDT today is most commonly used as a treatment for skin cancers and precancers, including squamous cell carcinoma (SCC) and basal cell carcinoma (BCC) which together comprise approximately 99% of all skin cancers (2) and present approximately 3.5×10^6 new cases annually (3). Actinic keratoses are preneoplastic lesions that lie on a continuous spectrum from early to late (invasive) SCC and at approximately 40×10^6 cases/year, actinic keratoses represent an even larger healthcare burden than the skin cancers themselves (3). Both actinic keratoses and early-stage skin cancers can be significantly ameliorated using PDT (4, 5).

PDT, a relative newcomer to cutaneous oncology, must be evaluated in comparison with more conventional therapies, including surgical excision, cryotherapy (liquid nitrogen), ionizing radiation, and topical chemotherapeutic agents such as 5-fluorouracil (5-FU). On the plus side, PDT has several major advantages over other standard-of-care therapies. First, unlike surgery or cryotherapy, PDT does not cause scarring (6, 7). Second, unlike ionizing radiation, PDT is non-mutagenic because it primarily affects the mitochondria rather than DNA (1), and can therefore be repeated indefinitely. Finally, unlike extended applications of 5-FU (8), PDT involves only about a week of posttreatment discomfort and rarely causes blistering nor post-inflammatory pigmentation. PDT is therefore a superior option for many patients with actinic keratoses, especially severely sun-damaged Caucasians and immunosuppressed organ transplant recipients who experience a high frequency of skin cancer (9). In head-to-head comparisons of PDT versus 5-FU, or versus cryotherapy, PDT was superior to either 5-FU or cryotherapy for widespread actinic keratoses (10, 11). For fully developed skin carcinomas, however, PDT cannot always match the cure rates after surgical excision. Most available data on PDT and skin cancer come from Europe, where PDT is licensed for treatment of BCC and SCC. Although 5-year cure rates after PDT for superficial BCC are reported in the 85% to 90% range in several European studies (refs. 12, 13; approaching surgical cure rates of >90%), cure rates for nodular BCC are slightly worse (60%–90%) and are considerably worse for invasive SCC (<60% complete cures; ref. 14). Even for

[1]Department of Biomedical Engineering, Cleveland Clinic, Cleveland, Ohio. [2]Department of Dermatology, Cleveland Clinic, Cleveland, Ohio. [3]Departments of Therapeutic Radiology and Dermatology, Yale School of Medicine, New Haven, Connecticut. [4]Wellman Center for Photomedicine, Massachusetts General Hospital, Boston, Massachusetts.

Note: Supplementary data for this article are available at Molecular Cancer Therapeutics Online (http://mct.aacrjournals.org/).

Corresponding Authors: Sanjay Anand, Cleveland Clinic, 9500 Euclid Avenue, Cleveland, OH 44195. Phone: 216-444-7015; Fax: 216-444-9198; E-mail: anands@ccf.org; and Edward V. Maytin, maytine@ccf.org

doi: 10.1158/1535-7163.MCT-16-0608

precancerous lesions (actinic keratoses), clearance rates after a single PDT treatment are typically only approximately 70% to 80% at 3 months (14), leaving some room for improvement. However, given that no existing modality gives a 100% cure, PDT offers special value as a scar-free alternative and would clearly be preferred if its efficacy were equivalent to surgery.

Major research efforts in PDT over the past decade have focused upon understanding biological responses of target tumors and host tissues (e.g., vascular responses) to PDT, and how to modulate these responses (15, 16). Our laboratory focused on the problem of photosensitizer heterogeneity. In solid tumors, many cells fail to produce sufficient PpIX to reach the threshold for photo-killing, a major liability in thick tumors where photon penetration is limited by tissue depth. As a potential solution, we pioneered "combination PDT" or combination photodynamic therapy (*cPDT*), an approach in which biological agents are used as neoadjuvants to increase PpIX accumulation before light delivery (17). Agents discovered to work well for this purpose were methotrexate (MTX; ref. 18) and Vitamin D (Vit D; calcitriol; ref. 19). When administered to tumor-bearing mice for 3 days before ALA on the fourth day, these cPDT pretreatments raise PpIX levels and increase tumor cell death as compared with PDT alone (18, 19). MTX and calcitriol were each found to enhance the differentiation state of cancer cells while stimulating PpIX production (17), a link that was seemed enigmatic but now appears to involve the concurrent expression of heme synthetic enzymes and genes associated with cellular differentiation, each governed by C/EBP transcription factors which are themselves regulated by MTX and calcitriol (20, 21).

MTX and calcitriol, two familiar drugs in widespread clinical use, would seem to be excellent candidates for cPDT. However, both agents present serious drawbacks when considering clinical trials. MTX causes liver toxicity, a risk that is generally low in healthy individuals but could become significant in a large population of skin cancer patients. Calcitriol, the active hormonal form of Vitamin D, can induce hypercalcemia when given systemically, and topical calcitriol is not approved by the FDA for skin cancer. Looking for alternatives, we realized that 5-FU might fulfill a need. 5-FU, a synthetic pyrimidine analogue, has been used for over 50 years for colon cancer and other carcinomas and is FDA-approved as a topical treatment for actinic keratoses (22). 5-FU and MTX share a common mechanism of action, inhibition of the pyrimidine salvage pathway. In this article, we show that 5-FU can enhance PpIX accumulation and improve therapeutic responses of squamous tumors using the cPDT approach.

Materials and Methods

Cell culture

A431, a human epidermoid carcinoma, and 4T1, a murine breast carcinoma line, were purchased from the ATCC and cultured as per the instructions provided (18). Cell lines were tested and authenticated at the ATCC by morphologic appearance during growth and recovery, cytochrome *c* oxidase 1 PCR for species specificity, and human origin by short tandem repeat (STR) profiling.

Murine models of cutaneous squamous cell carcinoma

All animal procedures were approved by the IACUC at Cleveland Clinic. The following mouse models of SCC were utilized: (i) UVB-induced actinic keratosis/SCC in mouse skin: SKH-1 mice were exposed to UVB for 20 weeks starting, at 90 mJ/cm^2 dose with a gradual 10% weekly increment, reaching a final dose of 180 mJ/cm^2. Hyperproliferative, actinic keratosis–like lesions began appearing on the dorsal skin around week 15, progressing to SCC-like lesions by week 25 (23). (ii) Subcutaneous SCC model: human A431 cells (2×10^6) were resuspended in a 1:1 mixture of growth medium:Matrigel (BD Biosciences) and injected into the flanks of female nude mice (Charles River Laboratories). (iii) Breast tumor model: murine 4T1 cells (0.5×10^6) were resuspended in 1:1 mixture of medium:Matrigel and injected into breast fat pads of female nude mice.

Pretreatment with 5-fluorouracil

Tumors generated by UVB carcinogenesis were preconditioned with 5-FU topical solution 2% w/w (Taro Pharmaceuticals) daily for 3 days. Petroleum jelly was applied as vehicle control. ALA (5-amino-4-oxopentanoic acid; Levulan Kerastick, DUSA/Sun Pharmaceuticals) was topically applied, and 4 hours later PpIX fluorescence in the tumors was analyzed by Maestro EX IVIS system. In separate experiments, tumors were either exposed to light for PDT treatment, or harvested (after euthanasia) for PpIX analysis by confocal microscopy. For subcutaneous A431 and 4T1 tumors, 5-FU (Sigma Aldrich, 300 mg/kg) was given by intraperitoneal injection daily for 3 days; control mice received PBS injections. On day 4, ALA was administered intraperitoneally (200 mg/kg in PBS) for 4 hours and the mice were either exposed to light for PDT, or euthanized for tumor harvest and further analyses.

In vivo imaging of PpIX using Maestro EX IVIS

PpIX-specific fluorescence in UVB-induced superficial tumors was analyzed with a Maestro EX IVIS *in vivo* imaging system (PerkinElmer). Anesthetized mice were placed in the device and fluorescence images obtained in 10 nm steps (500–720 nm range) using a blue filter set (excitation, 435–480 nm; emission 490 long pass). Fluorescence images from absolute control mice were used to determine the autofluorescence from experimental mice. Spectral unmixing and image processing were done using Maestro 3.0 Image Processing software, following the manufacturer's established protocol. PpIX fluorescence from individual tumors was quantitated using IP Lab software (Spectra Services) and expressed as fold change over vehicle control. More details on this technique can be found in Rollakanti and colleagues (24).

Photodynamic therapy

Anesthetized mice with superficial (UV-induced), A431, or 4T1 tumors, ± 5FU pretreatment and after 4 hours of ALA (5-ALA/5-Amino-4-oxopentanoic acid), were exposed to 100 J/cm^2 of 633 nm light using a LumaCare xenon source (LumaCare). The light source was calibrated using a FieldMate laser power meter (Coherent). Mice were sacrificed and tumors harvested at times shown in the figures.

Analysis of intratumoral PpIX by confocal microscopy

Cryosections (10 μm) of tumors embedded in OCT (Sakura Finetek) were placed on glass slides, briefly air-dried, mounted under coverslips with Vectashield (Vector Laboratories), and viewed on a confocal microscope (Leica Microsystems; ×40

magnification; excitation at 635 nm and image collection at 650–780 nm). Corresponding phase contrast images were captured for reference. Quantitative analysis of PpIX levels was performed, as described previously (18).

Histology, immunohistology, and cell death analyses

Tumors were harvested, formalin-fixed, paraffin-embedded, and sectioned (5 μm). Standard hematoxylin and eosin (H&E) staining, immunofluorescence staining, and cell death analysis (TUNEL) were performed as described previously (19). Sources and dilutions of primary and secondary antibodies were: E-Cadherin, p53, p21, MDM2 and GAPDH (Santa Cruz Biotechnology; 1:100), Ki-67 (NeoMarkers; 1:250), CY3-conjugated donkey anti-rabbit IgG (Jackson ImmunoResearch; 1:1,500), Alexa Fluor-488 conjugated goat anti-mouse IgG (Invitrogen; 1:1,000). Analysis of expression levels for all markers was performed using IPLab software (19).

Western blot analysis

Frozen tumors were crushed, dissolved in urea lysis buffer, and analyzed on Western blots as described previously (19). Source and dilutions of primary and secondary antibodies were: ALA dehydratase (ALAD; Abnova; 1:1,000), coproporphyrinogen oxidase (CPO; custom made, details in; ref. 25); 1:5,000), ferrochelatase (a gift of Dr. Harry Dailey; 1:5,000), glyceraldehyde 3-phosphate dehydrogenase, p21, p53, MDM2 (Santa Cruz Biotechnology; 1:5,000), porphobilinogen oxidase (PBGD, Abnova; 1:1,000), peroxidase conjugated goat anti-rabbit immunoglobin G (Jackson Immunoresearch; 1:20,000).

Results

Combination photodynamic therapy with 5-fluorouracil enhances PpIX levels in SCC tumors *in vivo*

Hairless mice with superficial, UVB-induced tumors were treated topically for 3 days with 5-FU or vehicle, followed by ALA application on the 4th day and estimation of intratumoral PpIX levels using noninvasive imaging (Fig. 1A). Relative to vehicle alone, 5-FU pretreatment led to higher PpIX levels along the dorsal surface where most tumors were present (Fig. 1A; bottom). For PpIX quantification, the location of each tumor in the bright-field images (Fig. 1A, top) was mapped onto the fluorescence images (Fig. 1A, bottom), and fluorescence intensity per tumor was analyzed via image processing. Pooled analyses revealed a 2.2-fold increase in PpIX due to 5-FU pretreatment (Fig. 1B). Those results were validated using an independent method in which PpIX in biopsies was assessed via confocal microscopy (Fig. 1C and D); this approach revealed a 3.5-fold PpIX enhancement due to 5-FU. In previous studies using MTX or calcitriol, a 3-4 fold increase in PpIX levels resulted in up to 5-fold increase in cell death in cells or tumors receiving cPDT (18, 19, 26).

To examine 5-FU's effects in a different skin cancer model, human A431 squamous carcinoma cells were implanted subcutaneously, and mice with visible and palpable tumors (Fig. 1E) were preconditioned with systemically injected 5-FU, or with vehicle control, for three days followed by systemic ALA for 4 hours. Confocal microscopy of frozen tissues revealed a 4-fold increase in PpIX levels throughout the 5-FU–preconditioned tumors (Fig. 1F and G, first two bars). Notably, PpIX induction was tumor-selective because no PpIX increase was observed in surrounding normal tissues after 5-FU (Fig. 1G, last two bars).

5-FU pretreatment inhibits proliferation, enhances differentiation, and alters expression of key enzymes in the heme biosynthetic pathway

For 5-FU, a well-known mechanism of action is downregulation of DNA synthesis through inhibition of thymidylate synthase (TS) and *de novo* synthesis of thymidylic acid (27). However, a less well-recognized effect of 5-FU (and of methotrexate) is enhancement of epithelial cell differentiation (17). We examined effects of 5-FU by immunostaining A431 tumors with antisera to Ki67 and E-cadherin, markers of proliferation and differentiation, respectively. As predicted, 5-FU preconditioning led to an approximately 70% decrease in cell proliferation (Fig. 2A, top; Fig. 2B, left) and also to a large (9-fold) increase in E-cadherin expression (Fig. 2A, bottom; Fig. 2B, right). In UVB-induced superficial SCC tumors, the effects of 5-FU upon differentiation were similar to effects in the subcutaneous A431 model (Supplementary Fig. S1).

To examine how 5-FU affects the enzymatic pathway responsible for PpIX production, lysates from vehicle- or 5-FU–treated A431 tumors were analyzed for expression of four key heme-synthetic enzymes (25): ALA dehydratase (ALAD), porphobilinogen deaminase (PBGD), coproporphyrinogen oxidase (CPO), and ferrochelatase (FC). In different biological systems, differences in expression of one or more of these four enzymes have been suggested as rate-limiting factors governing PpIX levels. Here, by Western blot analysis, three enzymes (ALAD, PBGD, and FC) showed a decrease in protein expression, whereas CPO expression was increased after 5-FU pretreatment (Fig. 2C, left vs. right). Densitometric quantification of the Western blots showed a 2-fold decrease in ALAD, a 4-fold decrease in PBGD and a 4-fold decrease in FC in 5-FU- versus vehicle-pretreated tumors. One enzyme, CPO, was increased 1.7-fold (Fig. 2D). Both the increase in CPO and the decrease in FC seem particularly relevant, because each change is expected to favor enhanced PpIX synthesis. This is because CPO and FC are located immediately upstream and downstream of PpIX, respectively, in the heme-synthetic pathway (25).

Enhanced PpIX in 5-FU pretreated A431 tumors correlates with increased tumor cell death following PDT

Subcutaneous tumors were harvested after ALA-mediated PDT to assess intratumoral cell death using TUNEL (i.e., labeling of cleaved internucleosomal DNA fragments). 5-FU–pretreated tumors showed a 16-fold increase in TUNEL-positive nuclei by 24 hours post PDT (Fig. 3A). This level was much greater, three times higher in fact, than after PDT alone (Fig. 3B).

To further characterize effects of cPDT, H&E-stained sections from tumors treated with PDT ± 5-FU were compared (Fig. 3C). During the 24 hours following PDT, all tumors developed many apoptotic cells with shrunken, pyknotic nuclei, extravasated red cells, intracellular vacuoles, and large areas of cell loss (empty spaces); these features were more pronounced in the 5-FU–pretreated tumors (Fig. 3C). To quantify these changes, loss of overall staining intensity (hypochromicity, reflecting a loss macromolecular synthesis) was analyzed from high-resolution digital micrographs (Fig. 3D). The distribution of brightness intensities, proportional to loss of staining, was calculated on a per-pixel basis and showed a shift to higher values over 24 hours post PDT

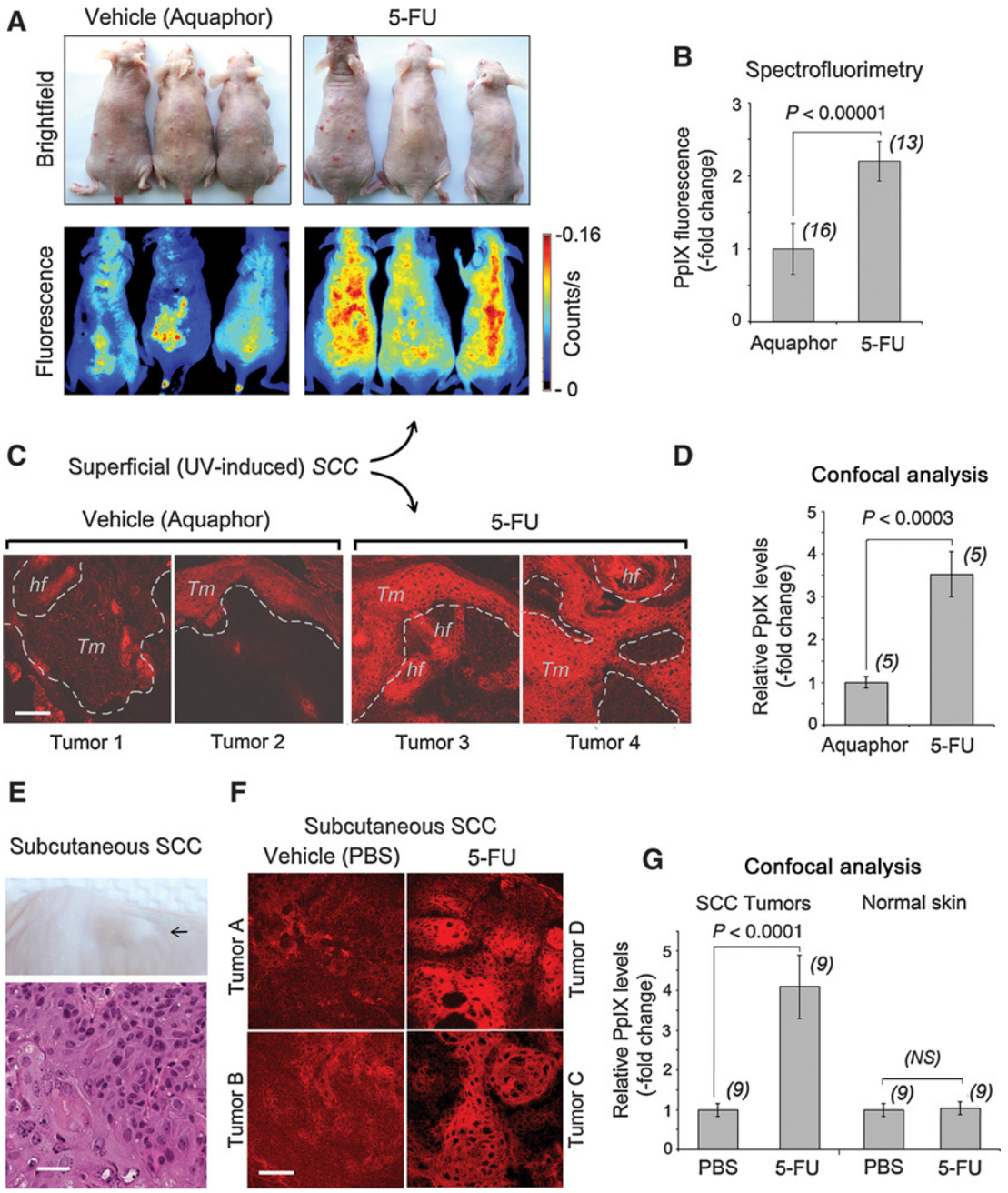

Figure 1.

5-FU pretreatment enhances PpIX production in superficial and subcutaneous SCC tumor models in mice. **A,** *In vivo* imaging of PpIX fluorescence in UVB-induced superficial SCCs in SKH-1 mice using Maestro EX IVIS. Tumors were treated topically with either Aquaphor (inert petrolatum; left column) or 5-FU topical solution (2% W/W; right column) once daily for 3 days, followed by topical application of ALA (Levulan Kerastick) on day 4 to stimulate PpIX synthesis. Top, photographs of SKH-1 mice showing UVB-induced tumors on their backs. Bottom, fluorescence intensity maps showing PpIX distribution in the skin of the same mice. **B,** Quantitation of PpIX-specific fluorescence levels in tumors. From Maestro EX IVIS fluorescence images, image cubes containing mixed signals (autofluorescence and PpIX-specific fluorescence) were unmixed to separate PpIX-specific signals, and individual pixel intensities were summed for each individual tumor. Mean ± SEM, with number of tumors in parentheses, are shown. **C,** Confocal micrographs of frozen tumor sections from superficial SCC, showing intracellular PpIX levels in four different tumors treated with Aquaphor (left column) or 5-FU (right column); representative examples are shown. Dotted line, boundaries of superficial papillomatous tumor. Tm, tumor. hf, hair follicle. **D,** Quantitation of PpIX signal from multiple tumors treated similarly to those in (**C**). **E,** Photograph showing a typical A431 subcutaneous tumor on a nude mouse. **F,** Confocal micrographs of frozen sections of different tumors that were treated systemically with either saline (left column) or 5-FU (right column); the observed signal is generated by PpIX. **G,** Quantitation of PpIX signal from multiple tumors, and from normal adjacent epidermis, using IP Lab software. Bars in **D** and **G** are mean ± SEM; number of tumors is indicated in parenthesis. *P* values from an unpaired two-sided Student *t* test are shown. Scale bars in (**C**, **E**, and **F**), 50 μm.

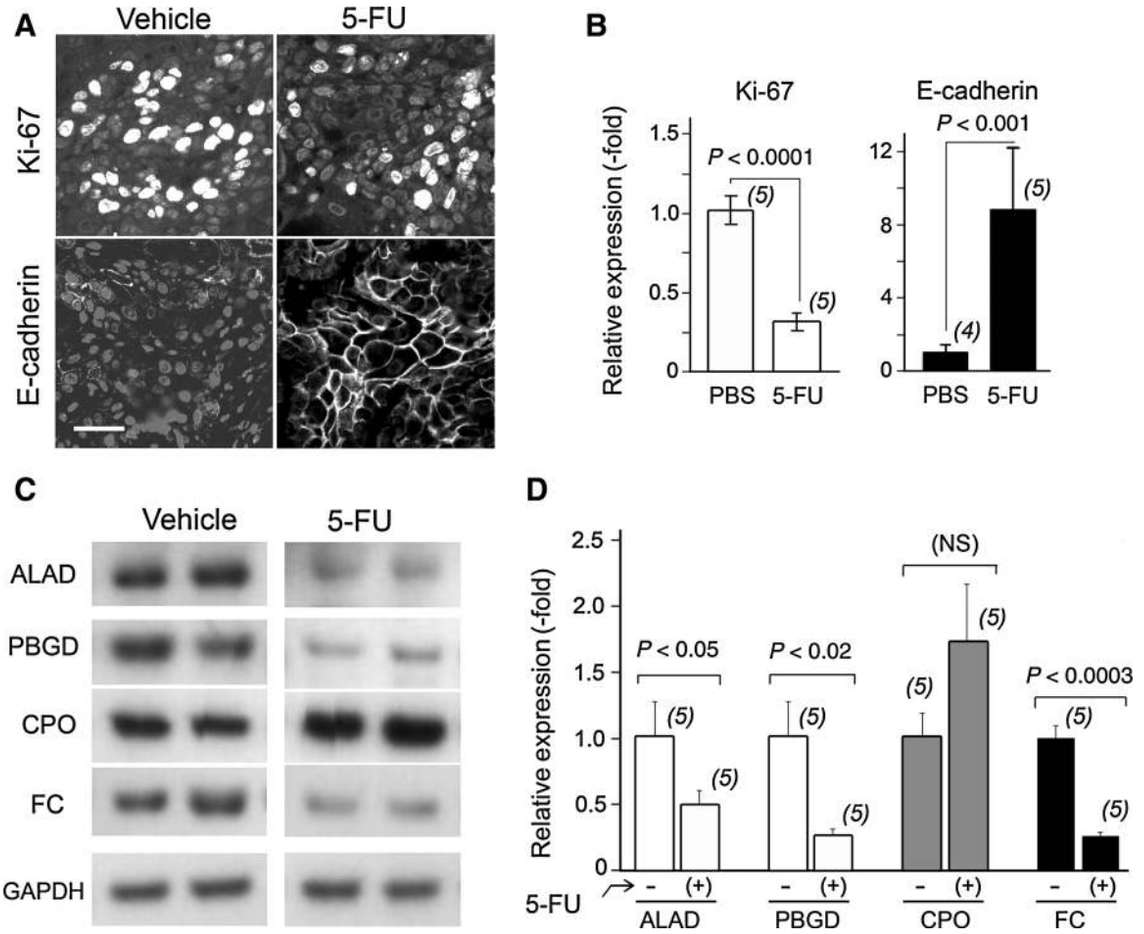

Figure 2.

Effects of 5-FU pretreatment on proliferation, differentiation, and heme enzyme levels in A431 tumors. **A,** Immunofluorescence microscopy images of A431 tumors, showing changes in proliferation (Ki-67) and differentiation (E-cadherin) in response to 3 days of pretreatment with vehicle (left column) or 5-FU (right column). Sections were counterstained with a nuclear dye, DAPI (grey); Scale bar, 50 μm. **B,** Quantitative analyses of relative expression levels of Ki-67 (left) and E-cadherin (right), analyzed from images similar to those in (**A**), using IP Lab software. Bars show mean ± SD; *P* value from two-sided unpaired *t* test. **C,** Expression of key enzymes in the heme-biosynthetic pathway, analyzed by Western blot analysis. Examples of Western blots from tumor lysates treated with vehicle or 5-FU and visualized with antisera to ALAD, PBGD, CPO or FC, or to GAPDH as an invariant control. **D,** Densitometric quantitation of relative expression levels of heme enzymes, normalized to GAPDH; blots from 5 individual tumors in each treatment group were analyzed; mean ± SD, *P* value from two-sided unpaired *t* test.

(Fig. 3D, top row). This shift was more pronounced in 5-FU–pretreated tumors (Fig. 3D, bottom row). Another aspect of this analysis was hypocellularity (empty white spaces indicative of cell death and tissue loss), represented by a sharp peak at the right of each graph (Fig. 3D, arrowheads); this peak became very large in 5-FU–pretreated tumors (Fig. 3D and E). The 3-fold enhancement in hypocellularity (Fig. 3E) agreed very well with approximately 3-fold enhancement in apoptosis seen with TUNEL (Fig. 3B). Thus, in two separate analyses (TUNEL and H&E), cPDT induced significantly more tumor destruction than PDT alone. Similar results were obtained in our UVB-induced mouse model of superficial SCC (Supplementary Fig. S2).

In A431 tumors, p53 protein is elevated after 5-FU pretreatment

To explore possible mechanisms of how 5-FU augments PDT-induced apoptosis, we asked whether caspase activation is involved because in a previous study (using calcitriol before ALA-based PDT of A431 tumors) we had observed activation of a TNFα-mediated, caspase-8 and caspase-3–dependent apoptotic pathway (the extrinsic pathway; ref. 19). With 5-FU as the neoadjuvant, however, no changes in caspase-3 expression or cleavage were detected. This indicates that the proapoptotic mechanisms for 5-FU and calcitriol are different.

p53 is a strong candidate for involvement in apoptosis because it is well-established that during cancer therapy, 5-FU can activate p53 (27) and that antitumor and stress-related effects of 5-FU are produced when 5-FU is phosphorylated and converted into active metabolites such as 5-fluorouridine-5′-triphosphate (FUTP) and 5-fluoro-2′-deoxyuridine-5′-monophosphate (FdUMP), leading to their misincorporation into RNA and DNA, respectively (22). To examine 5-FU's effects upon p53 pathways in A431 tumors, we measured expression of three molecules: p53; p21 (a downstream transcriptional target of p53); and MDM2 (a negative regulator of p53). By immunochemical staining (Fig. 4A) and by Western blot

analyses (Fig. 4B and C), 5-FU was shown to elevate p53 protein levels as compared with vehicle alone. Expression of p21 was reduced and MDM2 was increased (Figs. 4A–C). The fact that MDM2 and p53 are both increased may be due to disruption of p53–MDM2 interaction, as a result of a recently reported interaction between p53 and PpIX (ref. 28; see Discussion). A time course experiment, spanning just before light exposure to 24 hours post-PDT, demonstrated that elevations in p53 are sustained for

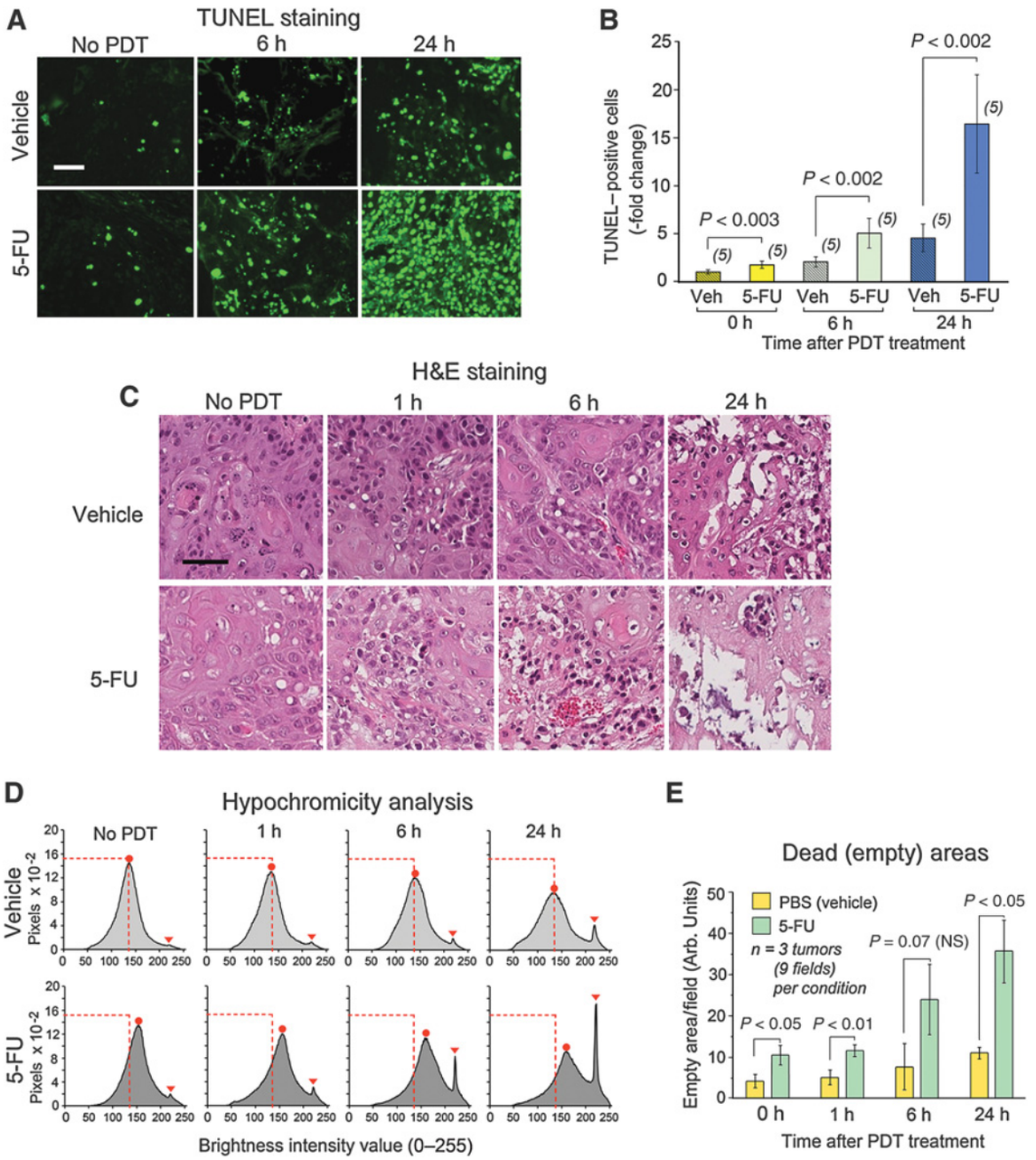

Figure 3.

Cell death analysis and quantitation in A431 tumors by TUNEL and by histomorphology of stained tissue. **A,** TUNEL-stained images showing selective enhancement of PDT-induced cell death in A431 tumors as a result of 5-FU pretreatment. TUNEL-positive nuclei in vehicle- (top) or 5-FU (bottom)–treated tumors either without PDT (left column) or 6 hours (middle column) and 24 hours (right column) post PDT; Scale bar, 50 μm. **B,** Quantitation of cell death time course in A431 tumors after pretreatment with vehicle or 5-FU. Mean ± SEM of number of tumors per treatment group (indicated in parenthesis); *P* values from an unpaired two-sided Student *t* test are shown. **C,** H&E-stained tumor sections showing time course of enhanced cell death following ALA-PDT in tumors pretreated with 5-FU (bottom) as compared with vehicle treated tumors (top); Scale bar, 50 μm. **D,** Quantitative analysis of loss of staining (as defined by pixel color intensity) in the digitized images shown in (**C**); see Materials and Methods for details and text for description. **E,** Quantitative analysis of dead area (white space) as a result of photodynamic destruction in the tumors from (**C**); mean ± SEM with *P* values from an unpaired two-sided Student *t* test.

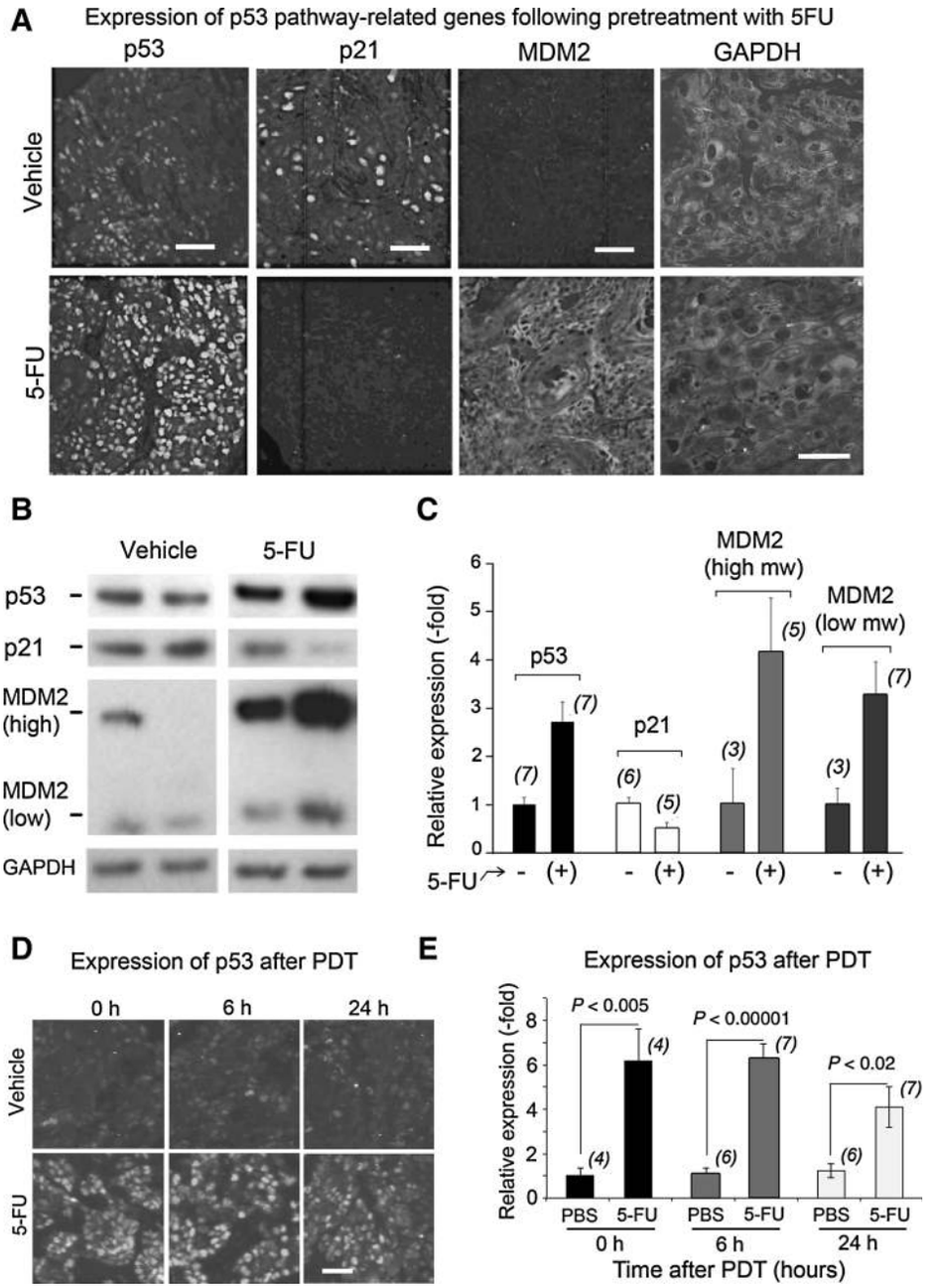

Figure 4.
Activation of p53 by 5-FU treatment in A431 tumors. **A,** Immunohistologic images showing expression of p53, p21, MDM2, and GAPDH in vehicle (top) or 5-FU (bottom) treated A431 tumors; Scale bars, 50 μm; **B,** Western blots showing expression levels of p53, p21, MDM2, and GAPDH in vehicle (left column) or 5-FU (right column)–treated A431 tumors. **C,** Quantitative densitometric analysis of relative expression levels of p53, p21, and MDM2 on Western blots, after normalization to GAPDH; the number of individual tumors per treatment group is indicated in parentheses. **D,** Immunohistological images showing a sustained increase in p53 levels during the time course following ALA-PDT in 5-FU–treated tumors as compared with vehicle treated tumors; scale bar, 50 μm. **E,** Quantitative analyses of relative p53 expression levels from the digital images in (**D**), using IP Lab software.

24 hours (Fig. 4D and E). The latter finding implies that in 5-FU preconditioned tumors, abundant p53 protein is available, and although mutated in this case, might contribute to enhanced apoptosis.

Absence of p53 expression reduces but does not eliminate the 5-FU–mediated induction of PpIX levels and cell death in tumors

To investigate whether the presence of p53 (or its increase after 5-FU) is a critical factor required to elevate PpIX levels in response to 5-FU, we used an epithelial cancer model in which p53 is completely absent. Mice bearing p53-null subcutaneous tumors (4T1 cells; $p53^{-/-}$) were pretreated with 5-FU, and the effects of 5-FU upon PpIX levels and PDT-induced cell death were examined. As compared with A431 tumors, the 5-FU pretreatment in 4T1 tumors led to smaller increases in PpIX pre-PDT (4-fold vs. 2.5-fold in Figs. 1G and 5A, respectively) and in cell death post-PDT (3.6-fold vs. 2.6-fold in Figs. 3B and 5B, respectively). These observations suggest that 5-FU's effect upon PpIX levels may be partially mediated through upregulation of p53, although it is somewhat difficult to make a definitive conclusion about this due to p53's mutated status in A431 cells. What is quite clear, however, is that p53 is not required to obtain a significant enhancement of PpIX levels and tumor cell death after PDT.

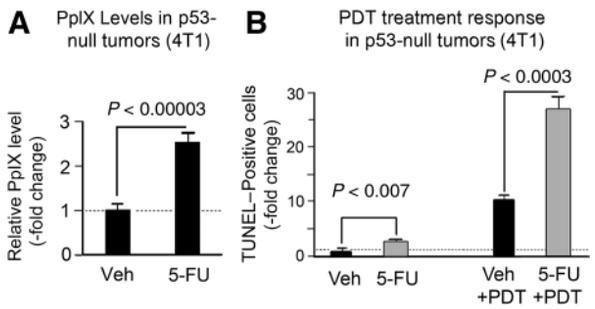

Figure 5.

Lack of p53 expression reduces but does not eliminate the 5-FU-mediated induction of PpIX levels and PDT-mediated cell death in squamous tumors. **A,** Effect of 5-FU pretreatment on PpIX levels in 4T1 ($p53^{-/-}$) breast tumors. Bars are mean ± SEM, $n = 6$ tumors/condition. **B,** Quantitation of cell death at 24 hours post PDT in 4T1 tumors after pretreatment with vehicle or 5-FU. Bars are mean ± SEM, $n = 4$ tumors/condition. *P* values from an unpaired two-sided Student *t* test are shown.

Discussion

In this study, we showed that pretreatment with 5-FU before PDT enhances the selective accumulation of PpIX and improves the cytotoxicity of PDT in epithelial tumors *in vivo*. Two different models were used for the initial demonstration of this effect: (i) an orthotopic skin cancer model, emulating human actinic keratoses and SCC induced by chronic UV exposure; (ii) human A431 (SCC) cells implanted subcutaneously in nude mice. In both systems, lesions pretreated with 5-FU showed tumor-selective PpIX accumulation in lesions (relative to surrounding normal skin), and these higher PpIX levels were associated with a significant increase in apoptosis after exposure to visible light with very little cell death in normal adjacent epidermis.

In addition to demonstrating the basic utility of 5-FU as a neoadjuvant for PDT, we have identified several different possible mechanisms for this therapeutic enhancement by 5-FU. The first was an inhibition of tumor cell proliferation (Fig. 2A), not surprising because 5-FU is known to inhibit thymidylate synthase as well as to produce metabolites that incorporate into DNA, and thereby cause growth arrest (22, 27). More novel was our demonstration that 5-FU stimulates tumor-selective increases in PpIX accumulation. Target tissue selectivity is a feature previously reported for other neoadjuvants such as methotrexate (18) and calcitriol in human psoriasis (29) and murine SCCs (24). Enhanced accumulation in tumor cells is important, but even more important may be the fact that 5-FU improves PpIX homogeneously within all cells in the tumor. For PDT to work well, a threshold concentration of the photosensitizer must be reached in every cell to achieve complete photodynamic killing. PpIX accumulation can vary so that some regions express almost no PpIX, as shown by a previous study in histologic sections of ALA-treated skin cancers (30). 5-FU addresses this problem by raising PpIX levels beyond the killing threshold in a high percentage of tumor cells, as shown by our confocal microscopic studies (Figs. 1C, and F).

To ask how 5-FU increases PpIX levels, we carefully examined the expression of selected key enzymes in the heme synthetic pathway to determine how they are altered by 5-FU. Eight enzymes are required for heme synthesis (summarized in; ref. 25) and six of these (ALAS, ALAD, PBGS, PBGD, CPO, and FC) have been studied in the literature in the context of ALA–PDT to assess their importance during ALA–PDT in different experimental contexts and cell types (17). In previous work on MTX or calcitriol as neoadjuvants, MTX preconditioning affected primarily CPO (18), whereas both CPO and FC were strongly affected after calcitriol (19, 26). In the current study, 5-FU led to increased CPO and decreased FC expression. ALAD and PBGD were also decreased, but those enzymes are expected to be less rate-limiting than CPO and FC which lie immediately upstream and downstream relative to PpIX in the heme pathway. Our results broadly agree with other studies performed by various groups using a gene-silencing approach, which amply demonstrated that downregulation of ALAD or PBGD reduced the PpIX levels, but silencing of FC was the only approach that elevated PpIX levels in target cells (31–33).

Another phenomenon we observed in this study, an increase in p53 in A431 tumors pretreated with 5-FU, was consistent with previous work showing that 5-FU exposure leads to incorporation of fluorodeoxyuridine triphosphate (FdUTP) into DNA, and fluorouridine triphosphate into RNA, triggering DNA-damage and RNA-damage responses, respectively (22, 34), thereby activating p53 (27). The observed p53 induction suggested to us another potential mechanism whereby 5-FU might contribute to PDT efficacy; it was formally possible, even though p53 is mutated in A431 cells (35), that this p53 might play some role in the observed enhancement of PpIX levels and subsequent cell death (36–38). To address the question of whether p53 induction plays an essential role or is just an epiphenomenon, we examined the PpIX and cell death levels in squamous tumors that are p53 null (the 4T1 tumor line). We found that 5-FU preconditioning can significantly induce PpIX accumulation and cell death even in the complete absence of p53 (Figs 5A and B). Thus, it appears that 5-FU can exert a PpIX-elevating effect through p53-independent mechanisms.

Although we have not definitively proven that p53 plays a role in the enhancement of PpIX-mediated PDT, the fact that inductions in PpIX levels and cell death in mutant p53-containing tumors was larger than in p53-null tumors (A431; Fig. 3B and 4T1; Fig. 5B, respectively), argues that a p53-mediated component of PpIX enhancement is still possible. One very intriguing piece of evidence in support of this notion is a series of reports showing that p53 can interact with PpIX, and perhaps stabilize it. Kaeser and colleagues (39) reported in HCT116 colon carcinoma cells that PpIX is able to bind p53. Later, Zawacka-Pankau and colleagues (28) showed that in cultured cells, PpIX binds to p53 at its N-terminus and disrupts the interaction between p53 and HDM2 (the human homolog of MDM2), thereby disrupting HDM2's negative regulation of p53 (40). If this scenario were operative in a given tumor cell, then a positive feed-forward loop might amplify 5-FU's proapoptotic effect, as elevated PpIX (caused by altered heme enzyme expression in 5FU-pretreated cells) would bind to p53, stabilize it, and thereby increase p53's ability to promote apoptosis after PDT damage. One uncertainty in A431 cells is the fact that A431 contain a mutant form of p53, one that fails to bind DNA and yet might still bind to other regulatory proteins and to PpIX. Although at first glance it might appear that the mutant p53 could not participate in mediating cell death, the complex nuances of p53 function deserve further discussion (see below).

We are certainly not the first investigators to wrestle with the question of whether PDT cytotoxicity is p53-dependent or

-independent. In fact, the role of p53 mutations as a determinant of p53's functional role in driving apoptosis after PDT is a rather thorny issue, with conflicting data in the literature. A role for p53 in PDT-induced cell death was reported by Fisher and colleagues (41) whereas other studies suggested that PDT responses were independent of p53 status (42, 43). The variety of different cells and photosensitizers makes those results difficult to interpret. In our study, the fact that A431 cells are known to express a common mutant of p53, called R273H (arginine-to-histidine missense mutation at codon 273) requires further discussion (35). Many p53 mutations, rather than causing a loss of tumor suppressor ability, actually acquire increased stability and exert dominant negative effects on wild-type p53, as "gain-of-function" mutants. In the case of p53 R273H, it was recently reported that the protein actually has antiapoptotic and antiautophagic activities, with tumors becoming even more resistant to cell death (44, 45). An article by Sznarkowska and colleagues suggests another possibility, namely, that cell death can be regulated by p73 (a p53 homolog that is rarely mutated in cancers and that binds to PpIX through its N-terminal domain, presumably stabilizing it.

Above and beyond the mechanistic details, a primary objective for this study was to obtain useful preclinical information for translation of improved cancer therapy to a clinical setting. Based upon these data in murine models, a clinical trial of combination therapy using neoadjuvantal 5-FU (ClinicalTrials.gov NCT01525329) has been designed, undertaken, and was recently submitted for publication (Maytin E, Anand S, and colleagues; unpublished observations). Results of that clinical trial confirm that 5-FU is a practical and effective neoadjuvant for PDT of early cutaneous neoplasia (actinic keratoses) in the skin. The 5-FU-plus-PDT combination regimen can be used immediately, because each of the individual modalities has a well-known safety profile and is already FDA-approved for the target indication (actinic keratoses). In the future, even greater benefits may become possible by further study of the basic mechanisms described here. Most promising is our finding that 5-FU–enhanced PDT appears to work even for p53-null tumors. The implication is that this approach may represent a promising alternative for a subset of cancers that is typically resistant to conventional chemotherapy and ionizing radiation.

Disclosure of Potential Conflicts of Interest

E.V. Maytin is a consultant/advisory board member for DUSA/Sun Pharmaceuticals (scientific advisory board). No potential conflicts of interest were disclosed by the other authors.

Authors' Contributions

Conception and design: S. Anand, N. Brankov, D.E. Brash, T. Hasan, E.V. Maytin
Development of methodology: S. Anand, N. Brankov, T. Hasan
Acquisition of data (provided animals, acquired and managed patients, provided facilities, etc.): S. Anand, K.R. Rollakanti, N. Brankov
Analysis and interpretation of data (e.g., statistical analysis, biostatistics, computational analysis): S. Anand, T. Hasan, E.V. Maytin
Writing, review, and/or revision of the manuscript: S. Anand, T. Hasan, E.V. Maytin
Administrative, technical, or material support (i.e., reporting or organizing data, constructing databases): T. Hasan
Study supervision: E.V. Maytin
Other (supported in funding): E.V. Maytin

Acknowledgments

We thank Judy Drazba, PhD, Director of the Lerner Research Institute Digital Imaging Core, for her outstanding dedication and service.

Grant Support

This work was supported by grant P01 CA084203 awarded to T. Hasan and E. V. Maytin from the National Cancer Institute, NIH.

The costs of publication of this article were defrayed in part by the payment of page charges. This article must therefore be hereby marked *advertisement* in accordance with 18 U.S.C. Section 1734 solely to indicate this fact.

Received September 12, 2016; revised October 7, 2016; accepted March 15, 2017; published OnlineFirst March 23, 2017.

References

1. Hasan T, Ortel B, Solban N, Pogue BW. Photodynamic therapy of cancer. In: Kufe DW, Pollock RE, Weichselbaum RR, Bast RC, Gansler TS, Holland JF, et al., editors. Cancer Medicine. 7th ed. Hamilton, Ontario: Decker, Inc.; 2006. pp. 537–48.
2. Rogers HW, Weinstock MA, Harris AR, Hinckley MR, Feldman SR, Fleischer AB, et al. Incidence estimate of nonmelanoma skin cancer in the United States, 2006. Arch Dermatol 2010;146:283–7.
3. Bickers DR, Lim HW, Margolis D, Weinstock MA, Goodman C, Faulkner E, et al. The burden of skin diseases: 2004 a joint project of the American academy of dermatology association and the society for investigative dermatology. J Am Acad Dermatol 2006;55:490–500.
4. Piacquadio DJ, Chen DM, Farber HF, Fowler JF Jr., Glazer SD, Goodman JJ, et al. Photodynamic therapy with aminolevulinic acid topical solution and visible blue light in the treatment of multiple actinic keratoses of the face and scalp: investigator-blinded, phase 3, multicenter trials. Arch Dermatol 2004;140:41–6.
5. Perrett CM, McGregor JM, Warwick J, Karran P, Leigh IM, Proby CM, et al. Treatment of post-transplant premalignant skin disease: a randomized intrapatient comparative study of 5-fluorouracil cream and topical photodynamic therapy. Br J Dermatol 2007; 156:320–8.
6. Campbell SM, Tyrrell J, Marshall R, Curnow A. Effect of MAL-photodynamic therapy on hypertrophic scarring. Photodiagnosis Photodyn Ther 2010;7:183–8.
7. Karrer S, Bosserhoff AK, Weiderer P, Landthaler M, Szeimies RM. Influence of 5-aminolevulinic acid and red light on collagen metabolism of human dermal fibroblasts. J Invest Dermatol 2003;120:325–31.
8. Stockfleth E. The paradigm shift in treating actinic keratosis: a comprehensive strategy. J Drugs Dermatol 2012;2012:1462–7.
9. Berg D, Otley CC. Skin cancer in organ transplant recipients: Epidemiology, pathogenesis, and management. J Am Acad Dermatol 2002; 47:1–17.
10. Salim A, Leman JA, McColl JH, Chapman R, Morton CA. Randomized comparison of photodynamic therapy with topical 5-fluorouracil in Bowen's disease. Br J Dermatol 2003;148:539–43.
11. Morton C, Horn M, Leman J, Tack B, Bedane C, Tjioe M, et al. Comparison of topical methyl aminolevulinate photodynamic therapy with cryotherapy or Fluorouracil for treatment of squamous cell carcinoma in situ: results of a multicenter randomized trial. Arch Dermatol 2006;142:729–35.
12. de Vijlder HC, Sterenborg HJ, Neumann HA, Robinson DJ, de Haas ER. Light fractionation significantly improves the response of superficial basal cell carcinoma to aminolaevulinic acid photodynamic therapy: five-year follow-up of a randomized, prospective trial. Acta Derm Venereol 2012;92:641–7.
13. Haller JC, Cairnduff F, Slack G, Schofield J, Whitehurst C, Tunstall R, et al. Routine double treatments of superficial basal cell carcinomas using aminolaevulinic acid-based photodynamic therapy. Br J Dermatol 2000; 143:1270–5.

14. Lehmann P. Methyl aminolaevulinate-photodynamic therapy: a review of clinical trials in the treatment of actinic keratoses and nonmelanoma skin cancer. Br J Dermatol 2007;156:793–801.
15. Spring BQ, Rizvi I, Xu N, Hasan T. The role of photodynamic therapy in overcoming cancer drug resistance. Photochem Photobiol Sci 2015;14: 1476–91.
16. Maas AL, Carter SL, Wileyto EP, Miller J, Yuan M, Yu G, et al. Tumor vascular microenvironment determines responsiveness to photodynamic therapy. Cancer Res 2012;72:2079–88.
17. Anand S, Ortel BJ, Pereira SP, Hasan T, Maytin EV. Biomodulatory approaches to photodynamic therapy for solid tumors. Cancer Lett 2012;326:8–16.
18. Anand S, Honari G, Hasan T, Elson P, Maytin EV. Low-dose methotrexate enhances aminolevulinate-based photodynamic therapy in skin carcinoma cells *in vitro* and *in vivo*. Clin Cancer Res 2009;15:3333–43.
19. Anand S, Wilson C, Hasan T, Maytin EV. Vitamin D3 enhances the apoptotic response of epithelial tumors to aminolevulinate-based photodynamic therapy. Cancer Res 2011;71:6040–50.
20. Anand S, Hasan T, Maytin EV. Mechanism of differentiation-enhanced photodynamic therapy for cancer: upregulation of coproporphyrinogen oxidase by C/EBP transcription factors. Mol Cancer Ther 2013;12: 1638–50.
21. Anand S, Ebner J, Warren CB, Raam MS, Piliang M, Billings SD, et al. C/EBP transcription factors in human squamous cell carcinoma: selective changes in expression of isoforms correlate with the neoplastic state. PLoS ONE 2014;9:e112073.
22. Tanaka F, Fukuse T, Wada H, Fukushima M. The history, mechanism and clinical use of oral 5-fluorouracil derivative chemotherapeutic agents. Curr Pharm Biotechnol 2000;1:137–64.
23. de Gruijl FR, van der Leun JC. Development of skin tumors in hairless mice after discontinuation of ultraviolet irradiation. Cancer Res 1991;51:979–84.
24. Rollakanti KR, Anand S, Davis SC, Pogue BW, Maytin EV. Noninvasive optical imaging of UV-induced squamous cell carcinoma in murine skin: Studies of early tumor development and vitamin D enhancement of protoporphyrin IX production. Photochem Photobiol 2015;91:1469–78.
25. Sinha AK, Anand S, Ortel BJ, Chang Y, Mai Z, Hasan T, et al. Methotrexate used in combination with aminolaevulinic acid for photodynamic killing of prostate cancer cells. Br J Cancer 2006;95:485–95.
26. Yang DF, Chen JH, Chiang CP, Huang Z, Lee JW, Liu CJ, et al. Improve efficacy of topical ALA-PDT by calcipotriol through up-regulation of coproporphyrinogen oxidase. Photodiagnosis Photodyn Ther 2014;11: 331–41.
27. Longley DB, Harkin DP, Johnston PG. 5-fluorouracil: mechanisms of action and clinical strategies. Nat Rev Cancer 2003;3:330–8.
28. Zawacka-Pankau J, Issaeva N, Hossain S, Pramanik A, Selivanova G, Podhajska AJ. Protoporphyrin IX interacts with wild-type p53 protein in vitro and induces cell death of human colon cancer cells in a p53-dependent and -independent manner. J Biol Chem 2007;282:2466–72.
29. Maytin EV, Honari G, Khachemoune A, Taylor CR, Ortel B, Pogue BW, et al. Vitamin D combined with aminolevulinate (ALA)-mediated photodynamic therapy (PDT) for human psoriasis: a proof-of-principle study. Isr J Chem 2012;52:767–75.
30. Warren CB. Prognostic markers for optimizing treatment after ALA photodynamic therapy of precancerous skin lesions and nonmelanoma skin tumors. Cleveland, OH: Case Western Reserve University; 2009.
31. Schauder A, Feuerstein T, Malik Z. The centrality of PBGD expression levels on ALA-PDT efficacy. Photochem Photobiol Sci 2011;10:1310–7.
32. Teng L, Nakada M, Zhao SG, Endo Y, Furuyama N, Nambu E, et al. Silencing of ferrochelatase enhances 5-aminolevulinic acid-based fluorescence and photodynamic therapy efficacy. Br J Cancer 2011;104: 798–807.
33. Yang X, Li W, Palasuberniam P, Myers KA, Wang C, Chen B. Effects of silencing heme biosynthesis enzymes on 5-aminolevulinic acid-mediated protoporphyrin IX fluorescence and photodynamic therapy. Photochem Photobiol 2015;91:923–30.
34. Ghoshal K, Jacob ST. An alternative molecular mechanism of action of 5-fluorouracil, a potent anticancer drug. Biochem Pharmacol 1997;53: 1569–75.
35. Reiss M, Brash DE, Munoz-Antonia T, Simon JA, Ziegler A, Vellucci VF, et al. Status of the p53 tumor suppressor gene in human squamous carcinoma cell lines. Oncol Res 1992;4:349–57.
36. Brash DE. Roles of the transcription factor p53 in keratinocyte carcinomas. Br J Dermatol 2006;154:8–10.
37. Muller PA, Vousden KH. Mutant p53 in cancer: new functions and therapeutic opportunities. Cancer Cell 2014;25:304–17.
38. Bieging KT, Mello SS, Attardi LD. Unravelling mechanisms of p53-mediated tumour suppression. Nat Rev Cancer 2014;14:359–70.
39. Kaeser MD, Pebernard S, Iggo RD. Regulation of p53 stability and function in HCT116 colon cancer cells. J Biol Chem 2004;279:7598–605.
40. Sznarkowska A, Malenczyk K, Kadzinski L, Bielawski KP, Banecki B, Zawacka-Pankau J. Targeting of p53 and its homolog p73 by protoporphyrin IX. FEBS Lett 2011;585:255–60.
41. Fisher AM, Danenberg K, Banerjee D, Bertino JR, Danenberg P, Gomer CJ. Increased photosensitivity in HL60 cells expressing wild-type p53. Photochem Photobiol 1997;66:265–70.
42. Fisher AM, Ferrario A, Rucker N, Zhang S, Gomer CJ. Photodynamic therapy sensitivity is not altered in human tumor cells after abrogation of p53 function. Cancer Res 1999;59:331–5.
43. Whitacre CM, Feyes DK, Satoh T, Grossmann J, Mulvihill JW, Mukhtar H, et al. Photodynamic therapy with the phthalocyanine photosensitizer Pc 4 of SW480 human colon cancer xenografts in athymic mice. Clin Cancer Res 2000;6:2021–7.
44. Tan BS, Tiong KH, Choo HL, Chung FF, Hii LW, Tan SH, et al. Mutant p53-R273H mediates cancer cell survival and anoikis resistance through AKT-dependent suppression of BCL2-modifying factor (BMF). Cell Death Dis 2015;6:e1826.
45. Thongrakard V, Titone R, Follo C, Morani F, Suksamrarn A, Tencomnao T, et al. Turmeric toxicity in A431 epidermoid cancer cells associates with autophagy degradation of anti-apoptotic and anti-autophagic p53 mutant. Phytother Res 2014;28:1761–9.